Fire Safety Journal 144 (2024) 104079

Contents lists available at ScienceDirect

Fire Safety Journal

journal homepage: www.elsevier.com/locate/firesaf

The influence of experimental conditions on the mass loss for TGA in fire safety science

K. De Lannoye [a,b], C. Trettin [c], A. Belt [a], E.A. Reinecke [b], R. Goertz [c], L. Arnold [a,d,*]

[a] Institute for Advanced Simulation, Forschungszentrum Jülich, Germany
[b] Institute of Energy and Climate Research, Forschungszentrum Jülich, Germany
[c] Chemical Safety and Fire Defence, University of Wuppertal, Germany
[d] Computational Civil Engineering, University of Wuppertal, Germany

ARTICLE INFO

Keywords:
TGA
PMMA
Pyrolysis
Heating rates
Atmospheres
Sample mass
Colour
Polymers

ABSTRACT

A thermogravimetric analyser (TGA) measures the mass loss of a sample as function of temperature, during a predefined heating program. The results are applied for developing reaction kinetics in fire safety science. It is assumed that the sample and the apparatus are in perfect thermal equilibrium. Therefore, the analysis ignores any apparatus or sample specific aspects. However, different experimental and material parameters, like the reacting atmosphere or sample mass, influence the observed mass loss. This research work illustrates the impact of experimental and material conditions on the measurement results. Polymethyl methacrylate (PMMA) is used for this study because of its important role in fire safety science. The influence of different atmospheres, sample mass, colour and flow rates was examined in three different TGA devices at heating rates between 2 K/min and 80 K/min. The major difference was observed for different atmospheres, inert versus synthetic air atmosphere. A difference up to 75 °C in onset temperature was found. The flow rate does not have any influence under inert atmosphere. The colour of the samples has a small influence on the mass loss rates. When comparing different devices, it was found that the peak temperature differs less than 10 °C under inert atmosphere. This contribution discusses and compares the observed influence of the different conditions.

1. Introduction

Thermogravimetric analysis (TGA) examines the chemical reactions and physical processes by analysing the time resolved mass loss of a sample under specific thermal conditions in an inert or oxidising atmosphere. The purpose of the TGA measurement is to characterise gasification reactions as function of sample temperature and time [1–4]. The significant quantity to specify the reaction kinetics is the time resolved mass loss. The use of TGA data in fire safety science is based on the idea that decomposition reactions can be identified, while thermal inertia (i.e. a temperature gradient within the sample) can be neglected. For obtaining representative mass loss results, different aspects must be considered. On the one hand the experimental conditions, like heating rate, atmosphere, inflow rate of gases, type of crucible (e.g. its material or diameter) must be defined. On the other hand the sample properties, like amount of material influence the mass loss. Several aspects have been studied in previous publications, e.g. molecular weight [5], heating rate [6], sample preparation [7].

In contrast to fire simulations, which are based on a prescribed design fire, the modelling of the flame spread involves chemical and physical processes in the solid, which emits the fuel. One of the main processes here is pyrolysis, which decomposes the solid material. It is common practice to describe the rate at which solid mass is converted into gas species with a set of Arrhenius equations. The involved parameters, i.e., the kinetic parameters for each reaction, are derived from the outcome of a TGA measurement. However, these parameters are not a direct output of a TGA measurement, but need to be derived from the data. For complex decompositions, an inverse modelling approach is needed, which uses the TGA data as target in an optimisation method. In the fire safety science community, this is a common method to find the kinetic parameters for flame spread simulations [8–10].

Independent of the used method to find the kinetic parameters, the characteristics of the mass loss rate curve have to be analysed. Before the inverse modelling [11] starts, the number of reaction steps is estimated, e.g., by the number of local maxima. In the common approaches, this needs to be done manually. Additionally, depending on the experimental conditions and the material, reactions can overlap, which makes this estimation more complex. In this process, it needs to be decided to what extent reaction steps with small peaks have to

* Corresponding author at: Institute for Advanced Simulation, Forschungszentrum Jülich, Germany.
E-mail address: l.arnold@fz-juelich.de (L. Arnold).

https://doi.org/10.1016/j.firesaf.2023.104079
Received 25 April 2023; Received in revised form 20 September 2023; Accepted 19 December 2023
Available online 21 December 2023

be taken into account — every considered reaction step increases the number of pyrolysis parameters. Consequently, the number of considered reactions influences directly the modelled flame spread, as small reactions, especially with low activation energies, may have a significant impact. By considering a higher number of endothermic reactions, the modelled flame spread in the fire simulation will be reduced or even limited. The quality of the TGA data and the above-mentioned decisions about the interpretation of mass loss can essentially influence the modelled fire scenario.

Furthermore, fire spread is a dynamical process, involving different atmospheres and heating rates [12]. For example, the material that is not yet burning will pre-heat and start to decompose under air atmosphere. While under the flame, the oxygen concentration is reduced. These different conditions should be taken into account when modelling fire spread. Therefore, the condition of the considered fire scenario must be transferred to the experimental configuration of TGA to determine the correct number of reaction steps as well as pyrolysis parameters.

In this research work, different experimental and material parameters influencing the mass loss results are examined. For this purpose, TGA experiments were conducted with polymethyl methacrylate (PMMA). The aim of this work is to show which parameters influence the results when conducting TGA experiments. In a next step it should than be considered what the influence of these changing results is on the parameters that are estimated based on TGA data, this is out of the scope of this contribution. PMMA was chosen due to its prominent role in fire safety engineering, e.g. [13]. Upon heating the PMMA surface melts, releasing pyrolysis gases which ignite. The flame radiation heats the surface, which continues to melt. This process takes place, because upon heating the PMMA releases monomer methyl methacrylate (MMA). The MMA decomposes further in smaller combustible products, which react with oxygen creating smaller molecules like CO_2, CO, H_2O, etc [14].

2. Method

For this work, experiments with three different apparatuses were conducted: a METTLER TOLEDO AG: TGA/DSC 1 (TGA M), a LINSEIS STA PT1600 (TGA L) and a SETARAM Themys duo TGA (TGA S). All three measure the mass loss of a sample during a defined temperature program, e.g. a linear increase of the temperature with a constant heating rate. Both TGA M and L are a combination of thermogravimetry and differential scanning calorimetry (DSC). All three TGAs have a different sample loading system. In Fig. 1,2 and 3 a schematic overview of the different TGA devices can be found. A sample is indicated in grey. The gas flow through the devices is shown by the dashed lines. Thermocouples measuring the assumed sample temperature are shown. Other thermocouples present in the device are not shown in the schemes. TGA M is a side-loaded TGA. Since it is a combined DSC system, it has one empty crucible (on the left) as reference for the DSC signal. The crucible on the right is filled with the sample. Both crucibles stand on the balance arm, which allows to measure the mass loss. TGA S has an electromagnetic suspension balance. This TGA consists of two identical ovens on both sides of a balance. The sample is placed in one of the ovens, while the other identical oven has an empty crucible. Buoyancy effects are compensated by the crucible in the counteracting empty oven. TGA L has a top load balance. The sample (on the right) and an empty reference crucible (on the left) are loaded from the top onto the balance. The empty reference crucible is for the DSC function of the device. In TGA M and TGA L, the thermocouples, measuring the sample temperature, are in contact with the crucible containing the sample. This is not the case for TGA S. Specifications of the furnaces and balance of the TGA's can be found in Table 1.

For the measurements, constant heating rates between 2 K/min and 80 K/min are chosen, since the heating rate influences the mass loss rates obtained from the TGA. In real scale fires broad ranges of heating rates can be found [15]. The samples are tested in a gas atmosphere similar to the ambient air atmosphere (21 vol % O_2 and 79 vol % N_2) and in an inert atmosphere (100 Vol % N_2 for TGA M and TGA L or Ar for TGA S). According to [6], under an inert atmosphere the composition of the inert gas does not influence the TGA results. Tests under air atmosphere were repeated at least three times, tests under inert atmosphere were repeated two or three times, unless explicitly mentioned otherwise. The recommended flow rates were used for the devices, this is 40 ml/min for TGA M and 20 ml/min for TGA S and TGA

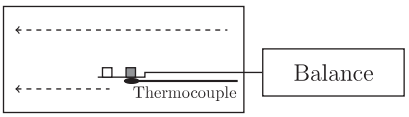

Fig. 1. TGA M: an empty crucible (left) and a crucible with sample (right) are placed on a horizontal balance arm. The gas flow through the device is indicated with the dashed lines.

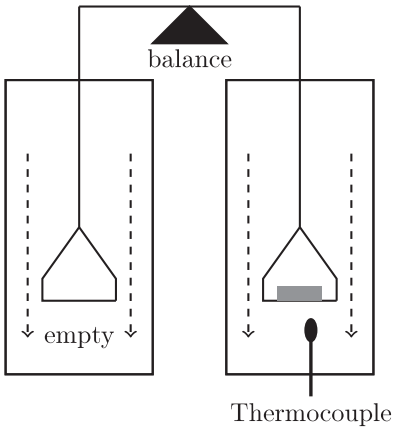

Fig. 2. TGA S: two identical ovens at both side of an electromagnetic balance (black triangle). In both ovens a crucible is suspended. In the right oven a sample is placed in the crucible. Both ovens have identical gas flows (indicated by the dashed lines).

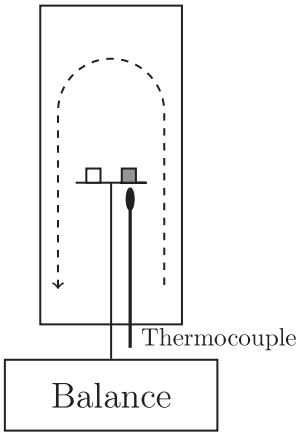

Fig. 3. TGA L: an empty crucible and a crucible with sample are loaded on a vertical balance arm. The gas flow through the device is indicated with the dashed lines.

Table 1
Specifications of the TGA's.

	TGA L	TGA S	TGA M
Oven diameter (mm)	28	18	20
Volume furnace (ml)	200	67	N/S
Balance capacity (mg)	25	20	5000
Balance sensitivity (μg)	0.5	0.002	1.0

Table 2
Reproducibility of the blank curves for TGA M and TGA L. Maximal difference between three repeated blank curves are shown (in mg). Only two repetitions are used for results marked with ∗.

Heating rate	TGA L Inert	TGA M Inert	TGA M Syn. air
2 K/min	–	0.0086	0.0040*
5 K/min	0.037	0.0084	0.015
10 K/min	0.022	0.10	0.12*
20 K/min	0.026	0.052*	0.095*
40 K/min	0.027	0.23	0.13*
60 K/min	–	0.016*	0.0025*
80 K/min	–	0.0070	0.0084

Table 3
Reproducibility of the PMMA experiments. Maximal difference between the normalised mass of three repetition measurements under inert atmosphere are shown. Only two repetitions are used for results marked with *.

Heating rate	TGA L	TGA S	TGA M
2 K/min	–	–	0.0079*
5 K/min	0.0077	0.0152	0.0085*
10 K/min	0.0099	0.0333	0.0233
20 K/min	0.0172	0.0131	0.0309
40 K/min	0.0105	–	0.0106*
60 K/min	–	–	0.0196*
80 K/min	–	–	0.0276

L. The reacting atmosphere represents the conditions before ignition and thermal processing without flame or ignition.

For the measurements, in TGA M, 70 µl aluminium oxide (Al_2O_3) crucibles with an inner diameter of 5 mm were used. In TGA L, aluminium oxide crucibles were used with a volume of 120 µl. In TGA S, a 130 µl platinum crucible was used. No lid was used in any of the experiments.

Buoyancy effects in a TGA apparatus will cause an apparent mass loss. These effects need to be compensated, in order to resolve the real mass loss of the sample. In TGA S this is done by the counteracting oven. Empty runs were performed to test the accuracy of this system. The mass for an empty run does not deviate more than $7 \cdot 10^{-3}$ mg. TGA L and TGA M only have one single oven. Blank curves need to be recorded in order to compensate for the buoyancy effects. This is a TGA run without sample under exactly the same conditions as the experiment. TGA data was corrected with the average of three blank curves, both for TGA M and L. Table 2 shows the maximal difference between three different empty repetitions for TGA M and TGA L.

The data sampling frequency is 1 Hz. This implies that in a fixed temperature range, higher heating rates have less data points than lower heating rates. This causes a natural smoothing for higher heating rates. The data originating from the measurements is the sample temperature and sample mass versus time. The mass loss data is derived over time to show the mass loss rate versus temperature. All result shown in this paper are normalised mass loss rates, using the total mass of the sample, and are labelled 'mass loss rate (1/s)'. Neither smoothing algorithm, nor a filter is applied to the displayed mass loss results. All results shown are averages of three measurements, unless explicitly stated otherwise. No error margin is displayed in the results because of the good reproducibility. Table 3 shows the maximum difference between three repeated experiments under inert atmosphere for TGA L (with PMMA 2020), TGA M (with PMMA 2016) and TGA S (with PMMA 2020).

Table 4 gives an overview of the different conditions that were examined, as is explained in the next section three different PMMAs were used. The results will be discussed in Section 4.

3. Sample material

All used PMMA is commercial, cast PMMA from Plexiglas®, by Evonik. Two types of black PMMA where used, both with product name

(a) Black PMMA from 2020 (b) Black PMMA from 2016 (c) Transparent PMMA

Fig. 4. Different TGA samples used in the experiments.

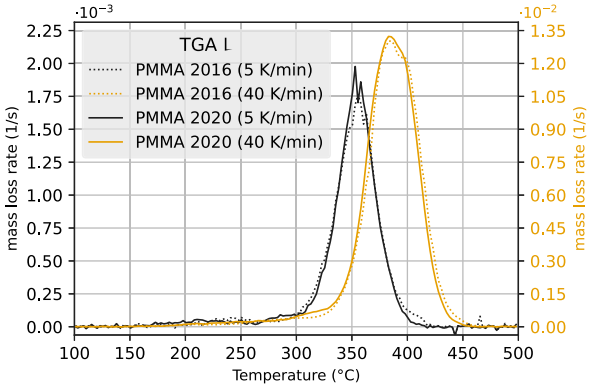

Fig. 5. Comparison between PMMA 2020 and PMMA 2016.

9H01, one was ordered in 2016 (with a plate thickness of 20 mm) and the second one was ordered in 2020 from 3 mm thick plates. The third type of PMMA is transparent, with product code 0F00, also ordered as 3 mm thick plates in 2020. Photographs of the different PMMA samples can be seen in Fig. 4(a), 4(b) and 4(c). The samples will be referred to as 'PMMA 2020' and 'PMMA 2016': for the black PMMA and 'PMMA Transparent' for the transparent samples. Elemental analysis has been conducted on all three sample types to determine the C,H, O content. The analysis was performed with a VarioLcube from Elementar [16], both in C,H,N mode and in O(xygen)-mode. For these measurements 2 mg samples were burned. The measurements were repeated three times for every mode and every sample type. The results of this analysis confirm that the atomic content of all three samples is the same (Table 5).

To produce sample thin slices were shaved of the PMMA block for the 20 mm thick material. For the 3 mm thick material, the material was milled down to a thickness of 5 mm. Samples were produced by pressing out thin slices of the PMMA with a hollow punch (diameter 4.5 mm for TGA M and 5 mm for TGA L and TGA S) and a hammer. Afterwards the circles were filed down to obtain the right mass. The thickness of the samples was altered by filing, the diameter did not change. A mass limit was based on the thermal characteristics such that mass and heat transfer can be neglected [17]. Samples with a mass of (8.50 ± 0.10) mg were tested, unless explicitly stated otherwise. The thickness was between 0.45 mm and 0.6 mm for the 4.5 mm diameter and around 0.4 mm for the 5 mm diameter samples. Both PMMA 2020 and PMMA 2016, which is the same product that has been ordered in different years, were analysed in the Linseis TGA to examine the similarity of the material. From Fig. 5 it can be seen that both materials exhibit a similar mass loss rate, apart from a small shoulder after the main reaction peak, explained in Section 4.2. The figure compares the materials for heating rates 5 K/min and 40 K/min. As stated in the previous section the displayed results are averages. The uncertainty on the averages is not shown because of the good reproducibility.

Table 4
Overview table of the experiments.

Conditions	TGA	Heating rate (K/min)	Atmosphere	Sample
Colour	S,L	5, 10, 20, 40	inert	PMMA 2020, Transparent
Flow rate	S,L	5, 40	inert	PMMA 2020, Transparent, PMMA 2016
Device	S,M,L	5, 10, 20, 40	inert	PMMA 2016, PMMA 2020,Transparent
Heating rate	S,M,L	2,5,10,20,40,60,80	inert, air	PMMA 2016, PMMA 2020,Transparent
Mass	M	5, 10, 20, 40, 60	inert, air	PMMA 2016
Atmosphere	M	2, 5, 10, 20, 40, 60, 80	inert, air	PMMA 2016

Table 5
C,H,O composition of the different sample materials.

Sample	C (wt%)	H (wt%)	O (wt%)
PMMA 2020	60.0 ± 0.2	7.86 ± 0.06	32.3 ± 0.1
PMMA 2016	59.8 ± 0.1	7.96 ± 0.03	32.5 ± 0.2
PMMA T	59.9 ± 0.1	7.98 ± 0.02	32.3 ± 0.1

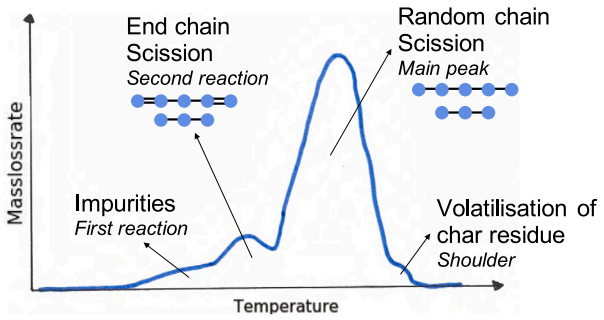

Fig. 6. Schematic of reactions observed in PMMA decomposition under nitrogen atmosphere.

4. Results

From literature, it is known that under inert atmosphere PMMA decomposes in 3 to 4 reaction steps [5,18], of which two smaller reaction peaks occur before a main decomposition reaction. This is schematically shown in Fig. 6. The samples studied in this contribution show one or two, depending on the conditions, smaller reactions prior to the main mass loss rate. Under some conditions the samples exhibit a small shoulder behind the main peak. For example Fig. 9 shows the four distinct reactions described in the literature. The first smaller peak is caused by impurities in the sample [18–20]. The second smaller peak is caused by end chain scission of the PMMA bonds. The main decomposition peak of PMMA is due to random chain scission of the polymer chain. According to [18,21] the shoulder behind the main peak is due to volatilisation of char residues.

It has been shown that under air atmosphere, the decomposition starts later [18]. The reactions caused by the impurities and end chain scission cannot be distinguished. The decomposition starts immediately with the main peak, caused by random chain scission. Below a temperature of 230 °C, oxygen increases the stability of the polymer. While, above this temperature it enhances the decomposition [18].

Under air atmosphere, it is observed that PMMA forms bubbles during decomposition in the TGA. In Fig. 8 pictures of PMMA samples are shown, where bubble formation can be seen. The pictures are taken at different temperatures and for different sample masses. The pictures were made by heating the samples in the TGA at a heating rate of 5 K/min. At the temperature indicated bellow the picture, the TGA was opened and the sample was photographed. The sample was than removed from the TGA and photographed again under a magnifier glass. No difference was observed between the pictures in the TGA and the ones under the magnifier glass. Therefore the later are shown. Non of the TGA devices allowed live visual monitoring of the sample. Under inert atmosphere the samples were not visually investigated. Therefore,

(a) PMMA 2020 (b) PMMA 2016 (c) Transparent

Fig. 7. Sample crucible with residue after an experiment under inert atmosphere.

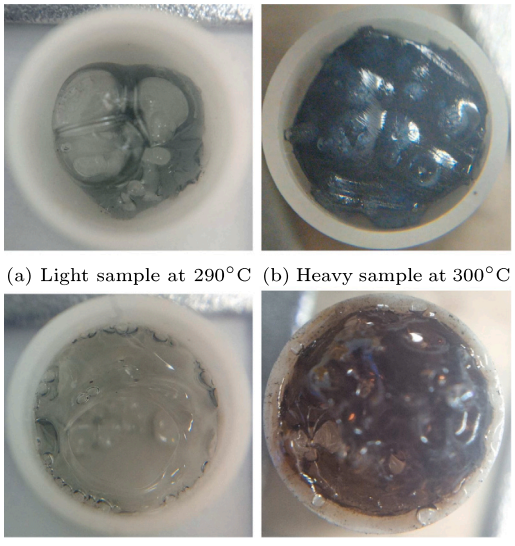

(a) Light sample at 290°C (b) Heavy sample at 300°C

(c) Light sample at 310°C (d) Heavy sample at 372°C

Fig. 8. Bubble formation for small (approx 8.5 mg) and large samples (approx. 75 mg) under air atmosphere.

no statement can be made on the presence of bubbles. Nevertheless, based on literature [22,23] and the observation of bubbles in other inert experiments with PMMA, it is expected that under inert atmosphere bubbles are also formed.

At the end of the experiment a negligible amount of residue was found in the crucibles for experiments under inert atmosphere. This can be seen in Fig. 7 for the three different kinds of PMMA. Note that black residue is also found for transparent samples. This indicates that the residue is not purely consisting of the colouring agent added to the black samples. Under air atmosphere no residue was found.

4.1. Different measurement devices

As outlined in Section 2, three different TGA devices were used to characterise the effect of the measurement devices. The biggest difference between the apparatuses is the orientation of the oven and the suspension of the balance.

Comparison between TGA M and TGA L was done with PMMA 2016 under nitrogen atmosphere and for four different heating rates: 5; 10; 20; 40 K/min.

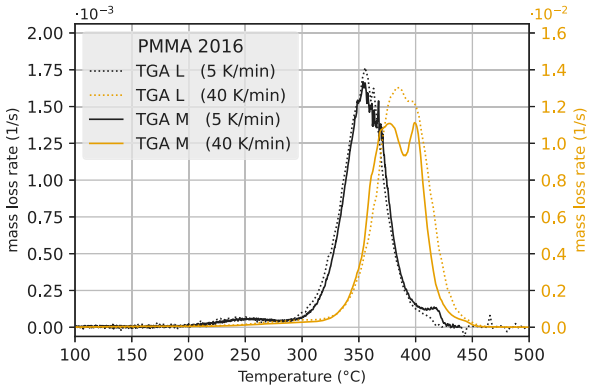

Fig. 9. Comparison between TGA L and TGA M.

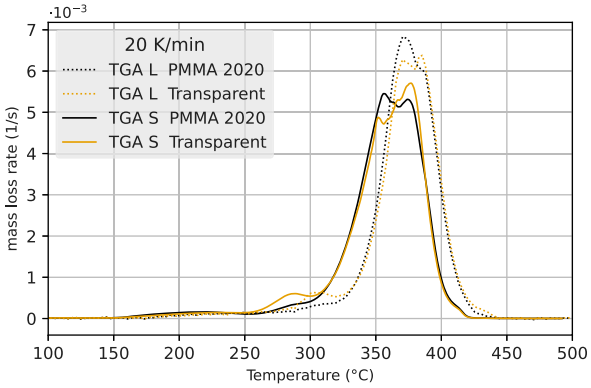

Fig. 10. Comparison between TGA S and TGA L.

Comparison between TGA L and TGA S was made with PMMA 2020 under inert atmosphere: nitrogen in TGA L and argon in TGA S. In TGA L, alumina crucibles were used, while in TGA S a platinum crucible was utilised. Three different heating rates were tested: 5; 10; 20 K/min. The comparison between TGA M and TGA L is shown in Fig. 9 for 5;40 K/min. Fig. 10 shows the differences between TGA L and TGA S both for transparent and PMMA 2020 samples.

For 5 K/min the behaviour of the samples in TGA M and TGA L is almost identical, except for a small shoulder between 400 °C and 450 °C. For 40 K/min the mass loss rates in both devices show significant differences. The maximum mass loss is higher for TGA L, while the width of the peak mass loss rate is slightly larger for TGA M. Additionally, TGA M has two clearly distinguishable peaks in the main reaction, while for TGA L the peaks are merged together. This suggests that the main mass loss is caused by multiple reactions. Looking in detail to the top of the main peak of TGA L, shows that this peak might also consist out of two distinct reactions merged together. The difference in shoulder, between 400 °C and 450 °C, disappears for higher heating rates. In contrast, the difference in main peak becomes larger for higher heating rates. For TGA S and TGA L, the qualitative behaviour of the samples remains the same up till 400 °C, i.e. form of the main peak, presence of the reactions before the main peak, etc. The mass loss rate measured by TGA S is shifted by 20 °C to 30 °C to lower temperature compared to TGA L. The maximum mass loss rate is higher for TGA L. The temperature shift between both devices becomes larger for higher heating rates.

Since the comparisons were carried out with the same sample material, it is excluded that differences in the mass loss rate are caused by a difference in reagent in the chemical reactions.

Due to the different layouts of the ovens, see Figs. 1, 2, 3 the radiation fraction received by the sample, originating from the oven walls might be different. The TGAs have a different gas inlet and different flow directions, which might also result in differences in convective cooling by the gas. The carrier gas in the oven transports heat from the oven wall to the sample. It might be that at higher heating rates the gas temperature becomes less homogeneous, causing temperature gradients between the TGA thermocouples and the samples.

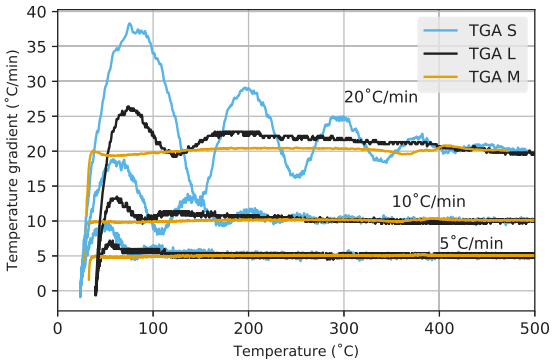

Fig. 11. Temperature gradient for different heating rates and different devices.

Fig. 11 shows the derivative of the measured temperature against time. As can be seen from the figure both TGA L and TGA M approximate well the ideal heating curve, while for TGA S there are stronger deviations from the desired heating rate. For 5 K/min and 10 K/min the heating rates of TGA S are relatively stable above 300 °C, where the main reaction is taking place. For 20 K/min however there are still deviations of around 5 K/min at 300 °C. This in combination with the different location of the thermocouple might be the cause of the offset in temperature between TGA S and TGA L. For TGA L and TGA M the thermocouple is located directly under sample, which is not the case for TGA S. Additional, crucibles made out of a different materials were used in the comparison between TGA S and TGA L. Platinum crucibles used in TGA S, have a heat capacity that is 7 times smaller than the aluminiumoxide crucibles in TGA L. This might also influence the heating rate received by the sample.

To summarise, the most relevant differences between the results of different devices are

- Difference in peak height and width of the mass loss rate
- Offset in reaction temperature
- Number of reactions (in main mass loss rate peak)

4.2. Different sample colour

To determine the effect of sample colour on the mass loss rate, TGA experiments were performed both with transparent and black PMMA samples. Black PMMA is favoured in fire safety research due to its high absorption coefficient, while transparent PMMA is more often used in applications, e.g. as replacement for glass. By testing both materials in the TGA it can be examined whether the absorption and emission properties of the sample influence the mass loss rate in small scale experiments. In the near infrared region, black PMMA has a 0% transmission degree, while transparent has a 85% transmission in this region [24]. Four different heating rates were tested under inert atmosphere: 5 K/min, 10 K/min, 20 K/min and 40 K/min. The mass loss results can be found in Fig. 12. For 5 K/min, the slow increase in mass loss between 150 °C and 250 °C is the same for both transparent and black samples (first reaction). Between 250 °C and 300 °C the transparent samples have a significantly higher mass loss rate than the black samples (second reaction). Between 300 °C and 400 °C both samples show a high increase in mass loss rate. At 400 °C transparent samples depict a small shoulder, which is not present for PMMA 2020. For 40 K/min the samples behave similar to 5 K/min

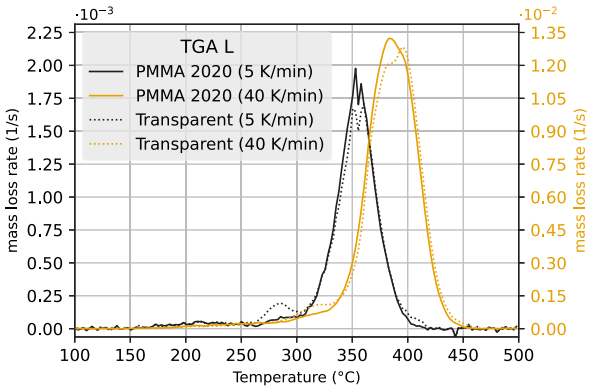

Fig. 12. Comparison between black (PMMA 2020) and transparent PMMA. (For interpretation of the references to colour in this figure legend, the reader is referred to the web version of this article.)

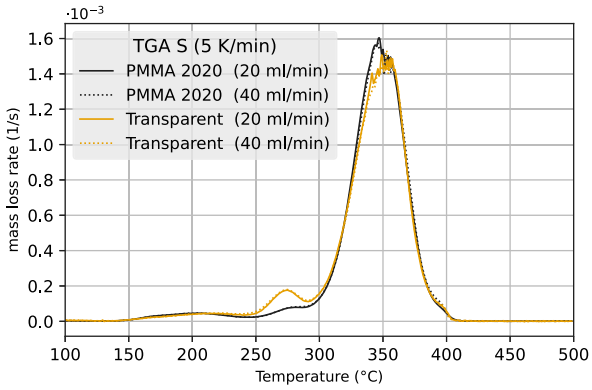

Fig. 13. Different flow rates in TGA S for 5 K/min.

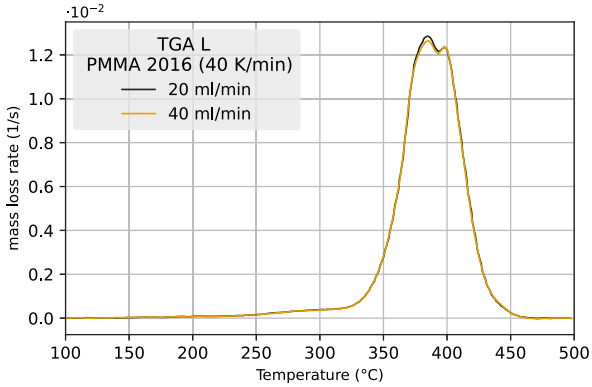

Fig. 14. Different flow rates in TGA L for 40 K/min.

where all peaks are shifted towards higher temperatures. The difference between transparent and black samples becomes smaller for the second reaction, while the main peak of the transparent sample seems to be shifted to higher temperatures. The shoulder after the main reaction peak disappears for higher heating rates. The mass loss rate of PMMA 2016 has a similar shoulder as transparent PMMA. From the sample pictures in Fig. 4, it can be seen that PMMA 2016 is more transparent than PMMA 2020. Therefore, it is expected that the shoulder behind the main peak is related to the transparency of the sample. Based on the colour or transparency of the sample, the absorption properties of the sample change. This shoulder is caused by the reaction of the char residue at the end of the decomposition process. To the authors knowledge, it is unknown whether there is a difference in amount of char formation between black and transparent PMMA.

The first small reaction in mass loss rate caused by impurities is the same for black and transparent PMMA. Transparent PMMA has a higher mass loss at the moment when end chain scission is taking place (second reaction). Consequently, in the main peak black PMMA has a slightly higher mass loss rate. Transparent and black plates are made of the same PMMA, the only difference is the addition of the colour-agent. Therefore it is unlikely that the difference in this peak is caused by difference in molecule length. For higher heating rates, end chain scission is not yet finished, when the sample is already hot enough to additionally start random chain scission. Consequently, the difference in the second reaction peak between transparent and black becomes smaller. This small peak is less distinguishable as a separate reaction. The main peak on the other hand seems to be made out of two phases from which one might be slightly dependent on the other. It could be the case that a different mechanism triggers the random chain scission causing different reaction peaks. It might be that one mechanism needs an educt of the first mechanism to trigger the random chain scission.

Consequently, for the pyrolysis modelling of different colours of PMMA the following aspects need to be considered

- Different number of distinguishable reactions
- Difference in maximum peak height

4.3. Different flow rate

The effect of the flow rate was examined for 5 K/min under argon atmosphere in TGA S and for 40 K/min in TGA L. In TGA S, this was done both for transparent PMMA and PMMA 2020. In TGA L, PMMA 2016 was used. The comparison is made between a flow rate of 20 ml/min and 40 ml/min.

The average results are shown in Figs. 13 and 14. As can be seen from the figure the flow rate does not have any significant influence on the behaviour of the mass loss rate within the same device under inert atmosphere. This is the case independent on the specific device, heating rate or type of PMMA sample. The flow rate was not varied under air atmosphere.

4.4. Different heating rates in inert atmosphere

The effect of different heating rates has often been studied in literature, e.g. [4,17,25]. For higher heating rates the mass loss curve shifts to higher temperatures and the reactions take place over a wider temperature range. The heating rate also influences the amount of reactions that can be distinguished [26], since high heating rates might result in overlapping reactions. Fig. 15 shows the effect of different heating rates on a theoretical Arrhenius equation:

$$\frac{d\alpha}{dt} = A\exp(-Ea/RT)(1-\alpha)^n, \tag{1}$$

where $alpha$ is the unreacted mass fraction, A is the pre-exponential factor, Ea is the activation energy and n is the reaction order. For the plot literature values for PMMA have been used: 200.4kJ/mol was used as activation energy; 10^{16} as pre-exponential factor and n was put to 1.21 [5].

Experiments were conducted for different heating rates for all devices, as is recommended by [17]. With TGA M seven different heating rates were tested: 2; 5; 10; 20; 40; 60; 80 K/min. Every measurement was repeated two times under nitrogen atmosphere.

Fig. 16 displays the mass loss rates for different heating rates. A comparison is made between 2;5; 10; 20; 40;60; 80 K/min.

For higher heating rates the mass loss curve shifts to higher temperature. Note that, especially at lower heating rates, the complete mass loss rate curve shifts, not only the temperature of the main peak. The main difference in mass loss rate for the different heating rates is in the main reaction. For higher heating rates the main reaction is more

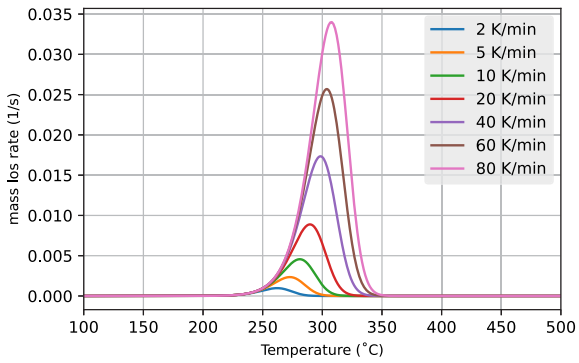

Fig. 15. The solution of the Arrhenius equation for different heating rates.

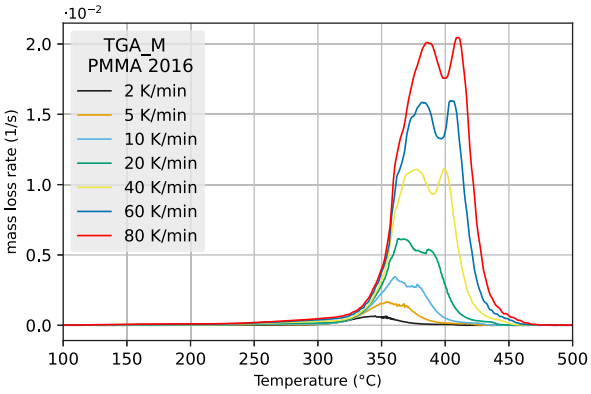

Fig. 16. Different heating rates under nitrogen atmosphere.

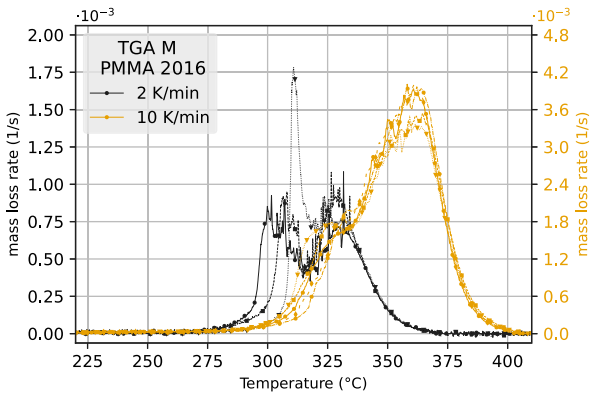

Fig. 17. 2 K/min and 10 K/min under synthetic air atmosphere.

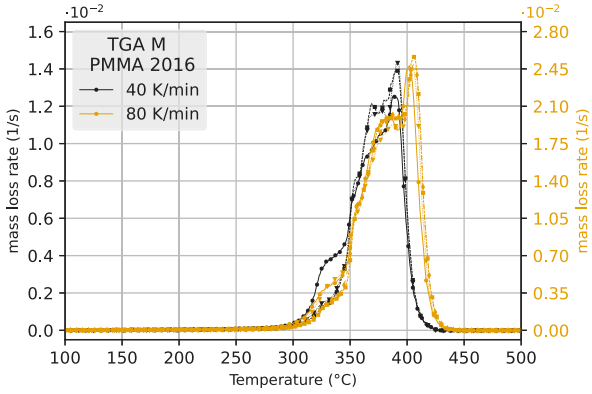

Fig. 18. 40 K/min and 80 K/min under synthetic air atmosphere.

and more manifested by two separate peaks, while for low heating rates only one peak is distinguishable. At lower heating rates the mass loss rate has a linear increase until the maximum value. For higher heating rates the increase of the mass loss rate becomes slower towards the maximum. The first reaction caused by the impurities becomes less present for higher heating rates. The same is valid for the shoulder, between 400 °C and 500 °C, behind the main peak: the higher the heating rate, the less present the shoulder is.

At this points we need to stress that at higher heating rates differences between TGA devices are more present, see Section 4.1. In the appendix, a comparison for different heating rates for TGA L can be found. For TGA L the division of the main peak into two reactions is less distinguishable. The shift towards higher temperatures for higher heating rates, the disappearing shoulder after the main peak and the less present peak caused by impurities can also be observed in TGA L.

Since the division in multiple reactions in the main peak is only present for one of the TGAs, this will not be discussed further. The reaction before the main peak gets less present for higher heating rates. Either, due to the high heating rate, the sample is not in thermal equilibrium, or the reaction could be time dependent (i.e. for slow reaction rates, the reaction just needs time to progress). This would imply that the reaction occurs too slowly and therefore interferes with the main peak. The main shift is most likely also caused by the sample not being in thermal equilibrium due to the high heating rate. According to Fig. 15, only a temperature shift in the main peak temperature and not in the onset temperature is expected in theory. As pointed out before, the shift in main peak is a known phenomena for TGA experiments. The shoulder behind the main peak gradually disappears for higher heating rates. The amount of char formed by the sample is small. Therefore the char is in thermal equilibrium, and starts reacting at the same temperature for every heating rate. Since the main peak is shifting towards higher temperatures, the char related shoulder becomes part of this main reaction for higher heating rates.

The effect of different heating rates can be summarised as follows. For higher heating rates

- the mass loss rate curve shifts towards higher temperatures
- the number of distinguishable reactions changes (e.g. main reaction, impurities)

4.5. Different heating rates in synthetic air

Experiments were performed for different heating rates under synthetic air atmosphere. All experiments were done with TGA M for 2; 5; 10; 20; 40; 60; 80 K/min. Every experiment was repeated at least three times.

The results are shown in Fig. 17,18 and 19. The individual experiments are plotted, because contrary to nitrogen atmospheres there is more variation between individual experiments.

The mass loss rate for low heating rates is less reproducible than for high heating rates. For low heating rates, e.g. 2 K/min and 5 K/min, two reaction peaks can be distinguished. There is a spread on the onset temperature of the first reaction phase between the different samples for one heating rate. When looking only at the mean values this would present itself wrongly as three reaction peaks. For 2 K/min, there is one measurement with a very high and steep first reaction peak. The end of the second reaction phase is at the same temperature for all samples.

For higher heating rates, the onset temperature of the first reaction phase is more alike between the different repetition experiments. The endset temperature is the same for all repetition experiments in one heating rate, even for low heating rates. For higher heating rates, the first main peak becomes less distinguishable. The increase towards the

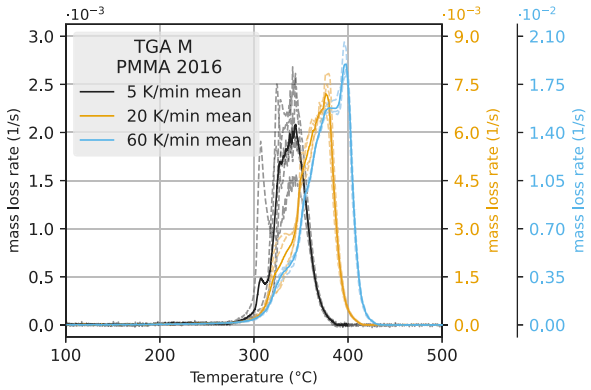

Fig. 19. 5 K/min, 20 K/min and 60 K/min under synthetic air atmosphere.

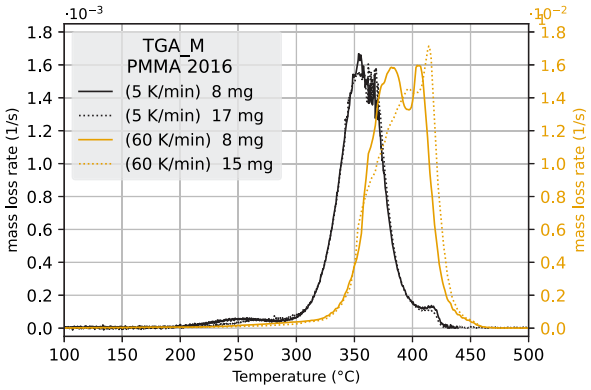

Fig. 20. Different sample masses for 5 K/min and 60 K/min under nitrogen atmosphere.

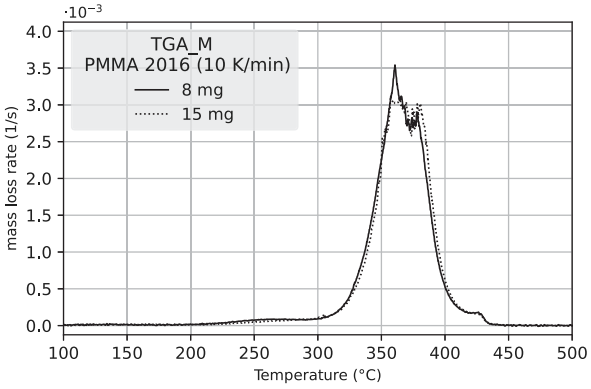

Fig. 21. Comparison between different masses for 10 K/min under nitrogen atmosphere.

main mass loss rate is less steep and takes place more step-wise. It can be seen that for intermediate heating rates, like e.g. 20 K/min, the first reaction phase is not present for every sample. While for higher heating rates, this first stage disappears completely. The second reaction phase becomes more a plateau. Starting from 10 K/min, more than two distinguishable reaction peaks can be observed. Additionally, the maximum mass loss rate shifts to higher temperatures for higher heating rates. The temperature range, in which the mass loss takes place, increases for higher heating rates. While, the last reaction stage becomes more separated.

Under thermal decomposition, PMMA forms bubbles in a random process. When a bubble pops this results in a sudden release of gas. Because of the small size of the PMMA samples and the momentum of a sudden release, this can have a strong effect on the mass loss.

Upon heating the surface of the PMMA samples melts. Around the melting temperature PMMA has a high viscosity [27]. It is known, that for liquids the viscosity decreases with temperature [28]. This effect is larger for more viscous liquids and has also been observed for dilute solutions of PMMA [29]. In other fields of research it has been shown, that in more viscous fluids smaller sized bubbles are formed than in less viscous fluids [30].

As the temperature becomes higher the PMMA becomes more viscous, allowing bubbles to form. The high heating rate causes inhomogeneities in the surface tension, which results in the bubbles releasing gas sooner due to shears compared to samples that heat up slower. The bubbles contain MMA gas. As the sample continues to be heated in the TGA, the gas inside the bubbles also gets heated. The higher the heating rate, the faster the gas in the bubble heats. This results in a higher pressure inside the bubble which also contributes to bubbles popping sooner for higher heating rates. Due to the oxygen in the surrounding atmosphere, the random chain scission process starts earlier [14,23]. Bursted bubbles leave holes, allowing a larger surface area of the sample to interact with oxygen. As a consequence, the reproducibility under oxygen atmosphere strongly depends on the bubble size and form. Therefore, these experiments show a worse reproducibility. The sudden mass loss for the outlier at 2 K/min could be caused by a bubble that suddenly pops. As explained these bubbles can become quiet large (compared to the sample size) for low heating rates, while the higher heating rates produce smaller bubbles. As the sample continues to heat it reaches the point where the viscosity becomes small enough to form bigger bubbles and the sharp increase to the main reaction peak starts.

Under air atmosphere, two competing process take place. Bubbles containing monomer MMA that is formed in the sample diffuse towards the surface, while oxygen diffuses into the sample. This competing interaction of the inward and outward diffusion, is time and temperature dependent. This could explain the more step-wise curves for higher heating rates.

As with inert atmosphere, the mass loss curves shift to higher temperature for higher heating rate. A shift in main peak, as can be observed when comparing 40 K/min and 80 K/min, is expected (see Fig. 15). However, when comparing 2 K/min and 10 K/min it can be seen that not only the temperature of the main peak shifts but e.g. also the onset temperature of the reactions. This is most likely also caused by the sample not being in thermal equilibrium due to the high heating rate.

Under synthetic air atmosphere the following observations should be considered when modelling or using TGA data

- The amount of reaction stages depends on heating rate
- On- and endset temperatures shift to higher values for higher heating rates.
- The temperature range of the reactions extends for higher heating rates
- Low heating rates have poor reproducibility

4.6. Different masses under inert atmosphere

There is no consensus on which sample mass to use for TGA analysis. Even the standard norms [1,2] do not provide a clear specification. The effect of sample mass has been examined in a dedicated study. For 5 K/min 8.5 mg and 17 mg were compared; for 10 K/min and 60 K/min, 8.5 mg and 15 mg. The 15 mg experiments were only conducted once. Experiments were conducted under nitrogen atmosphere in TGA M.

In Fig. 20 and 21 the results for 5 K/min and 60 K/min, respectively 10 K/min are shown.

Independent of the mass, the reactions start at the same temperature. As can be seen from the figure, there is very little difference

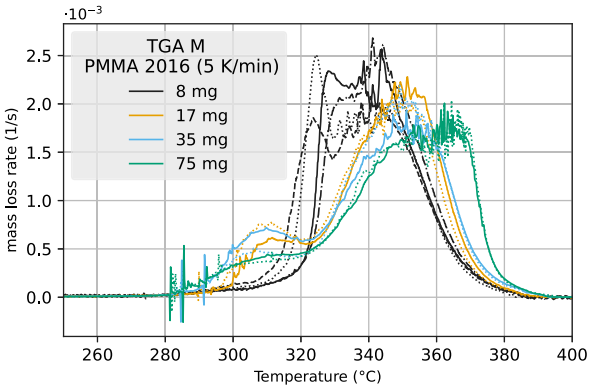

Fig. 22. Different sample masses for 5 K/min under synthetic air atmosphere. Individual experiments are plotted, using different line-styles. The colour of the lines correspond to the sample mass. (For interpretation of the references to colour in this figure legend, the reader is referred to the web version of this article.)

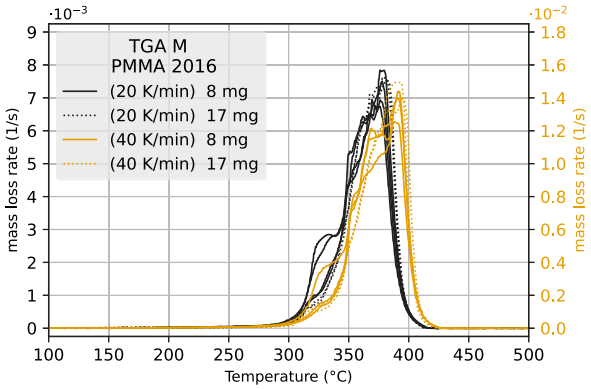

Fig. 23. Different sample masses for 20 and 40 K/min under synthetic air atmosphere. Individual experiments are shown, not the average.

between 8.5 mg and 17 mg for low heating rates. There might be a difference in the first reaction, but this is difficult to distinguish. For 10 K/min, the main peaks of heavier samples have a small shift towards higher temperatures. Otherwise the mass loss rate of both heavier and light samples are identical. For higher heating rates the difference in mass loss rate increases. Initially, the mass loss rate for higher masses increases strongly afterwards the increase becomes slower. The first part of the main peak merges more to the second part for heavier samples. Causing the first peak to be lower and the maximal mass loss rate to be higher. For lower masses, these two parts are separated. The peak width of both reactions widens for higher masses.

For higher heating rates and higher masses, the sample does not reach thermal equilibrium. This causes a part of the main peak to move to higher temperatures since the reaction temperature is not reached through out the full sample. Nevertheless, the onset temperature for the main peak is the same since the surface of the sample is sufficiently heated to start reacting. The main reaction peak is higher for heavier samples. The sample reaches the limiting temperature for random chain scission through out the whole sample, causing a faster mass loss and a higher main peak.

The effect of sample mass under inert atmosphere can be summarised by the following points:

- The sample mass has no influence for low heating rates;
- For high heating rates, the sample mass impacts the maximum mass loss rate as well as the amount of reactions needed to model the mass loss rate.

4.7. Different masses in synthetic air

Experiments were conducted with different masses under a synthetic air atmosphere with TGA M. For 5 K/min, the following masses were tested: 8.5 mg, 17 mg, 35 mg and 75 mg. For 20 K/min and 40 K/min, 8.5 mg and 17 mg were tested. The results of the experiments are shown in Figs. 22 and 23.

For the low heating rate (5 K/min), the first reaction phase starts earlier for higher masses. The first reaction phase for 8.5 mg starts at 320 °C, while for the other masses it starts already around 300 °C. For higher masses, the first reaction stage shows a slower increase while for lower masses the first reaction merges with the main peak. Both 35 mg and 75 mg have some noise in the start of the first reaction peak, as well as in the main peak.

The second reaction phase shows a slower increase for higher masses. Additionally, the maximum mass loss rate decreases with sample mass. For the highest mass, 75 mg, the second reaction phase reaches a plateau between 340 °C and 380 °C. At least two reactions would be needed to model this plateau form. The endset temperature is similar for all sample masses. The final decrease in mass loss rate is steeper for higher masses. The trend that is seen for higher masses with 5 K/min is similar to the trend seen for higher heating rates with 8.5 mg. However, the temperature shift present for the different heating rates is not present for the different masses. The reproducibility increases with higher masses.

For the high heating rates, 20 K/min and 40 K/min, the influence of the mass is smaller. It can be seen that the on- and endset temperature for the reactions is the same for all masses. Between the different masses, there is no temperature shift observed. The first reaction phase is not present for the higher masses, while for the lower mass for some samples it is present. The last reaction phase is less separated for higher masses. A nearly linear increase towards the main peak is observed for higher mass. At least two reactions would be needed to model this increase. The decrease after the maximum mass loss rate is steeper for higher masses.

As stated in Section 4.5, under air atmosphere MMA is released by the formation of bubbles. In Fig. 8, photographs are shown for different sample masses. Samples with a low mass get heated more uniform than samples with a high mass. This results in lower sample and surface,as heat is transported to the bulk of the sample, temperatures for heavier samples. Hence, the viscosity (at the surface) will be larger for lighter samples. The MMA bubbles that are formed inside the sample mitigate to the surface, where they can accumulate in larger bubbles. Due to the low viscosity, big bubbles can be formed. While heavier samples with a higher viscosity can only form smaller bubbles, since they will burst before reaching a big volume. Consequently, thicker samples start reacting earlier (see Fig. 22, at 290 °C). Additionally, for thinner (and therefore lighter) samples, the large surface to volume ratio allows a big part of the sample to interact with oxygen, which enhances the random chain scission. For low masses, the burst of one bubble, leads to a significant loss in mass. Additionally, space is freed in the sample through which oxygen can diffuse. This implies, that the release of one big bubble can enhance the random chain scission process. For higher masses, the formed bubbles are smaller. Since the amount of bubbles becomes larger, the reproducibility of the experiments becomes higher. During the heating of the sample, the viscosity becomes lower, resulting in larger bubbles for higher temperatures. The change in viscosity and bubble formation causes a small decrease in mass loss rate around 310 °C. Furthermore, the sample deforms due to the thermal stress, which influences its volume and consequently density. The noise within the main peak is attributed to the random process of larger bubbles bursting. The main peak gets wider, since for a heavier sample it takes longer before the oxygen can interact with the full sample. The cause of the signal noise for higher masses at the beginning of the first reaction is unclear.

When modelling TGA data under oxygen atmosphere, the following observations should be considered

Table 6
Main difference between samples tested under an inert atmosphere and samples tested under an air atmosphere.

Low heating rate
• Shoulder before main peak: only present under nitrogen atmosphere. • Main peak: one reaction phase under nitrogen atmosphere, at least two under air atmosphere. • Shoulder behind main peak: only present under nitrogen atmosphere.
High heating rate
• First part of main reaction peak have similar temperature and mass loss rate in nitrogen and air. • Second main part of main reaction peak is earlier for air.

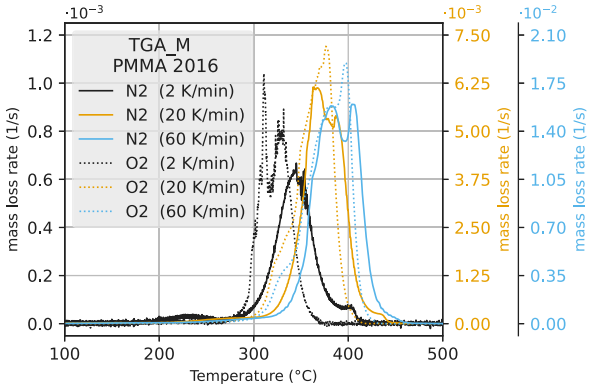

Fig. 24. Comparison between synthetic air and N_2 atmosphere.

- The number of distinguishable reaction phases changes with the sample mass
- The relative importance of the different reactions changes with the sample mass
- The maximum mass loss rate decreases for higher masses

4.8. Different atmospheres

Mass loss rate curves under inert and under synthetic air are compared in Fig. 24 for 2 K/min, 20 K/min, and 60 K/min.

The on- and endset temperature of the main reaction is different between both atmospheres for all heating rates. While the temperature range of the main reaction is similar under both atmospheres, the main mass loss rate of the sample starts earlier under oxygen atmosphere and has a steeper increase. The maximum mass loss rate is lower for samples heated under an inert atmosphere. In general, the mass loss curves from samples under inert atmosphere can be represented with fewer reactions than those under synthetic air atmosphere.

Table 6 summarises the differences between the samples behaviour under a synthetic air atmosphere and nitrogen atmosphere. A division is made between low (2 K/min and 5 K/min) and high heating rates (starting from 40 K/min). The mass loss rates for low heating rates under an air atmosphere are less reproducible as under an inert atmosphere. Therefore, the mean curves might show different characteristics and amounts of reaction phases due to the variation in individual mass loss curves. The behaviour for intermediate heating rates, like 10 K/min and 20 K/min, can be seen as a separator between the comparison for low and high heating rates. For example, for heating rates bellow 20 K/min, the samples under an inert atmosphere have a smooth increase towards the main peak. Whereby, reaction modelling for an air atmosphere would need multiple reaction phases to represent the increase towards the maximum.

The mechanisms triggering the scission process are different under air than under an inert atmosphere, therefore the mass loss curves are completely different. Under an inert atmosphere, the main process influencing the mass loss rate, is the diffusion of MMA towards the surface. Under an air atmosphere, the formation of MMA is influenced by the interaction of oxygen with the sample and therefore the diffusion of oxygen into the sample. Under an air atmosphere, the mass loss starts later, since no end chain scission is taking place due to the stabilising effect of oxygen at low temperatures. However, the main peak starts earlier due to the enhancing effect of oxygen at higher temperatures [23]. Under an air atmosphere, no shoulder originating from decomposition of char residues is present, since char is more reactive in the presence of oxygen.

When modelling TGA data, the following should be taken into account

- depending on the atmosphere, different processes take place
- Therefore, the mass loss rate for both atmospheres have significant deviations

4.9. Comparison

The effects of different conditions are compared, in Table 7, by calculating the root mean square error (RMSE) between the averaged normalised mass loss rates of both conditions, the difference in onset temperature, peak temperature and maximum mass loss rate. It is expected that for higher heating rates, the RMSE increases since the maximum mass loss rate increases. Within one column (i.e. one heating rate) one can compare which experimental or material parameters result in the largest difference in normalised mass loss rate.

Different atmospheres result in significantly different mass loss rates. Under air atmosphere, larger mass seem to result in larger differences in maximum mass loss rate as well as in peak temperature. However, due to the large uncertainty, especially on the 8.5 mg experiments at 5 K/min, all differences are within the uncertainty. Under nitrogen atmosphere large differences are found between TGA S and TGA L, as explained in 4.1 this is most likely due to the not well regulated heating rate of TGA S. When looking at the results of TGA M and TGA L, the biggest difference in maximum mass loss rate (up to 0.213 s^{-1}) for low heating rates (5 K/min) is caused by different sample colours. While the biggest offset in onset and peak temperature is between different mass at low heating rate. For high heating rates (40 K/min and 60 K/min), different devices cause the biggest difference in onset temperature (up to 29 °C) and maximum mass loss rate (up to 1.92 s^{-1}). While different masses cause the biggest difference in peak temperature (up to 21.5 °C). Note that in Table 7, the effect of the heating rate on maximum mass loss rate, peak temperature and onset temperature was not shown. As is well known from literature, for higher heating rates, the maximum mass loss rate and the peak temperature increase. This is also the case for the experiments conducted for this study, as was discussed in Sections 4.4 and 4.5.

5. Conclusion

In this paper, the influence of experimental settings on TGA experiments was discussed. Black and transparent PMMA from Plexiglas®, by Evonik, was used. Furthermore, products of different manufacturing years were considered.

The research work shows, that the number of decomposition reactions and the amount of mass loss depends on specific experimental

Table 7
Comparison of the different effects studied in this paper. RMSE values of the normalised mass loss rate have to be multiplied with a factor 10^{-6}. Difference in peak mass loss rate, indicated in 10^{-3}/s, difference in onset temperature (°C), difference in peak temperature (°C).

Effect	2 K/min	5K/min	10 K/min	20 K/min	40 K/min	60 K/min	80 K/min
Colour (TGA L):							
• RMSE	–	2.36	4.45	7.69	15.7	–	–
• Max MLR	–	0.213 ± 0.048	0.486 ± 0.123	0.417 ± 0.071	0.416 ± 0.122	–	–
• Onset T	–	1.0 ± 1.1	5.6 ± 9.4	1.2 ± 4.9	3.7 ± 3.9	–	–
• Peak T	–	4.2 ± 2.3	6.3 ± 3.8	8.5 ± 7.0	10.3 ± 1.7	–	–
Flow rate (TGA S):							
• RMSE	–	0.608	–	–		–	–
• Max MLR	–	0.055 ± 0.050	–	–		–	–
• Onset T	–	5.0 ± 1.8	–	–		–	–
• Peak T	–	2.4 ± 2.4	–	–		–	–
Flow rate (TGA L):							
• RMSE	–	–	–	–	4.51	–	–
• Max MLR	–	–	–	–	0.431 ± 0.231	–	–
• Onset T	–	–	–	–	24.0 ± 3.4	–	–
• Peak T	–	–	–	–	0.4 ± 0.8	–	–
Device:							
TGA L vs TGA M:							
• RMSE	–	2.26	3.06	11.8	41.2	–	–
• Max MLR	–	0.113 ± 0.030	0.107 ± 0.172	0.403 ± 0.097	1.920 ± 0.101	–	–
• Onset T	–	4.0 ± 2.2	4.0 ± 5.7	24 ± 14.0	29 ± 3.0	–	–
• Peak T	–	0.2 ± 1.1	2.6 ± 0.9	7.6 ± 2.7	4.4 ± 11.0	–	–
TGA L vs TGA S:							
• RMSE	–	5.20	12.7	35.0	–	–	–
• Max MLR	–	0.431 ± 0.025	0.687 ± 0.140	1.350 ± 0.115	–	–	–
• Onset T	–	30.2 ± 0.5	29.2 ± 9.0	20.2 ± 4.7	–	–	–
• Peak T	–	14.7 ± 3.6	8.7 ± 4.7	6 ± 2.1	–	–	–
Mass (inert):							
8.5 mg vs 17 mg:							
• RMSE	–	1.37	–	–	–	–	–
• Max MLR	–	0.023 ± 0.009	–	–	–	–	–
• Onset T	–	16.5 ± 2.3	–	–	–	–	–
• Peak T	–	10.8 ± 3.6	–	–	–	–	–
8.5 mg vs 15 mg:							
• RMSE	–	–	5.92	–	–	75.2	–
• Max MLR	–	–	0.414 ± 0.169	–	–	0.898 ± 0.149	–
• Onset T	–	–	3.2 ± 3.3	–	–	4.5 ± 0.5	–
• Peak T	–	–	2.2 ± 0.8	–	–	21.5 ± 11.5	–
Mass (air):							
8.5 mg vs 17 mg:							
• RMSE	–	11.3	–	16.2	27.7	–	–
• Max MLR	–	0.201 ± 0.354	–	0.265 ± 0.077	0.816 ± 0.927	–	–
• Onset T	–	13.2 ± 20.7	–	29.0 ± 13.8	14.3 ± 8.0	–	–
• Peak T	–	18.4 ± 16.8	–	5.9 ± 2.1	1.8 ± 2.3	–	–
8.5 mg vs 35 mg:							
• RMSE	–	12.3	–	–	–	–	–
• Max MLR	–	0.321 ± 0.364	–	–	–	–	–
• Onset T	–	14.9 ± 20.7	–	–	–	–	–
• Peak T	–	19.4 ± 16.7	–	–	–	–	–
8.5 mg vs 75 mg:							
• RMSE	–	16.2	–	–	–	–	–
• Max MLR	–	0.361 ± 0.341	–	–	–	–	–
• Onset T	–	15.4 ± 20.7	–	–	–	–	–
• Peak T	–	32.6 ± 16.7	–	–	–	–	–
Atmosphere							
• RMSE	7.05	17.5	20.3	32.9	59.5	85.3	82.9
• Max MLR	0.632 ± 0.330	0.688 ± 0.341	0.262 ± 0.283	0.989 ± 0.393	2.492 ± 0.790	2.867 ± 1.1	4.420 ± 0.778
• Onset T	74.4± .6	48.3 ± 20.7	51.2 ± 5.6	42.1 ± 16.2	45.7 ± 7.4	29.5 ± 8.8	32.2 ± 14.3
• Peak T	30.4 ± 8.9	23.8 ± 16.7	1.2 ± 2.4	11.0 ± 3.8	1.2 ± 11.1	4.8 ± 11.5	3 ± 11.5

conditions. Under nitrogen atmosphere, the colour effect is small, while the flow rate of the purge gas has no effect. For TGAs with a similar set-up, little difference is found between the measurement devices, especially for low heating rates. For high heating rates, differences occur in the main decomposition peak. Between different set-ups, it was identified, that the accuracy of the heating rate as well as of the thermocouple positions are responsible for differences in the results.

Under nitrogen atmosphere, changing the heating rate, as well as changing the mass, affects the main decomposition process. This is caused by the sample not being in thermal equilibrium. For higher heating rates, the main peak will be shifted to higher temperatures. For higher masses, the mass loss is slower until a limiting temperature is achieved, at which the mass loss accelerates.

The decomposition mechanism under synthetic air differs significantly from a measurement under nitrogen atmosphere, due to the enhancing effect of oxygen. MMA is released under the form of bubbles, which creates holes for oxygen diffusing into the sample. For low heating rates and small masses, a poor reproducibility is found, caused by the formation of big bubbles. For higher heating rates and high masses, multiple smaller bubbles are formed, improving the reproducibility and the amount of measurement noise.

Decomposition conditions change during the spread of a fire. The parts of the material that are not yet burning are heated up under air atmosphere. Under the flame, the oxygen concentration is reduced. Additionally, the heating rate increases under the flame. These different conditions were analysed in the TGA and influences illustrated. As results, it can be stated, that for fire spread modelling the different conditions should be considered depending on the modelled fire spread phase. Additionally, depending on the accuracy needed from the TGA data for estimating kinetic parameters for modelling, one needs to take into account parameters like the lay-out of the device. Most of the current models used for determining these parameters are over simplified and cannot take these effects into account.

CRediT authorship contribution statement

K. De Lannoye: Conceptualization, Methodology, Formal analysis, Investigation, Data curation, Writing – original draft, Writing – review & editing, Visualization. **C. Trettin:** Conceptualization, Methodology, Formal analysis, Investigation, Data curation, Writing – original draft. **A. Belt:** Writing – review & editing, Supervision. **E.A. Reinecke:** Resources, Funding acquisition, Writing – review & editing, Supervision. **R. Goertz:** Funding acquisition, Writing – review & editing, Supervision. **L. Arnold:** Funding acquisition, Writing – review & editing, Supervision.

Declaration of competing interest

The authors declare that they have no known competing financial interests or personal relationships that could have appeared to influence the work reported in this paper.

References

[1] Plastics — Thermogravimetry (TG) of Polymers — Part 1: General principles, Standard, European Standard, 2022.

[2] DIN 51006: Thermal analysis (TA) - Thermogravimetry (TG) - Principles, Standard, German National Standard, 2005.

[3] Thermal Analysis (TA) - Vocabulary, Standard, German National Standard, 2005.

[4] A.W. Coats, J.P. Redfern, Thermogravimetric analysis. A review, Analyst 88 (1053) (1963) 906.

[5] M. Ferriol, A. Gentilhomme, M. Cochez, N. Oget, J.L. Mieloszynski, Thermal degradation of poly(methyl methacrylate) (PMMA): modelling of DTG and TG curves, Polym. Degrad. Stab. 79 (2) (2003) 271–281.

[6] O.P. Korobeinichev, A.A. Paletsky, M.B. Gonchikzhapov, R.K. Glaznev, I.E. Gerasimov, Y.K. Naganovsky, I.K. Shundrina, A.Yu. Snegirev, R. Vinu, Kinetics of thermal decomposition of PMMA at different heating rates and in a wide temperature range, Thermochim. Acta 671 (2019) 17–25.

[7] Matthew J. DiDomizio, Mark B. McKinnon, Impact of specimen preparation method on thermal analysis testing and derived parameters, in: Morgan C. Bruns, Marc L. Janssens (Eds.), Obtaining Data for Fire Growth Models, ASTM International, 100 Barr Harbor Drive, PO Box C700, West Conshohocken, PA 19428-2959, 2023, pp. 64–87.

[8] Anna Matala, Methods and applications of pyrolysis modelling for polymeric materials.pdf.

[9] Tristan Hehnen, Lukas Arnold, Saverio La Mendola, Numerical fire spread simulation based on material pyrolysis—An application to the CHRISTIFIRE phase 1 horizontal cable tray tests, Fire 3 (3) (2020) 33.

[10] Alexandra Viitanen, Simo Hostikka, Jukka Vaari, CFD simulations of fire propagation in horizontal cable trays using a pyrolysis model with stochastically determined geometry, Fire Technol. (2022).

[11] Tristan Hehnen, Lukas Arnold, PMMA pyrolysis simulation – from micro- to real-scale.

[12] Morgan J. Hurley, Daniel Gottuk, John R. Hall, Kazunori Harada, Erica Kuligowski, Milosh Puchovsky, José Torero, John M. Watts, Christopher Wieczorek (Eds.), SFPE Handbook of Fire Protection Engineering, fifth ed., Springer New York, New York, NY, 2016.

[13] Benjamin Batiot, Morgan Bruns, Simo Hostikka, Isaac Leventon, Yuji Nakamura, Pedro Reszka, Thomas Rogaume, Stanislav Stoliarov, The MaCFP condensed phase working group - experimental, 2021.

[14] W.R. Zeng, S.F. Li, W.K. Chow, Review on chemical reactions of burning poly(methyl methacrylate) PMMA, J. Fire Sci. 20 (5) (2002) 401–433, Publisher: SAGE Publications Ltd STM.

[15] SFPE, SFPE Handbook of Fire Protection Engineering, fifth ed., Springer, 2016.

[16] Elementar, Vario El cube.

[17] Sergey Vyazovkin, Konstantinos Chrissafis, Maria Laura Di Lorenzo, Nobuyoshi Koga, Michèle Pijolat, Bertrand Roduit, Nicolas Sbirrazzuoli, Joan Josep Suñol, ICTAC Kinetics Committee recommendations for collecting experimental thermal analysis data for kinetic computations, Thermochim. Acta 590 (2014) 1–23.

[18] T. Hirata, Takashi Kashiwagi, J.E. Brown, Thermal and oxidative degradation of poly(methyl methacrylate): weight loss, Macromolecules 18 (7) (1985) 1410–1418, Publisher: American Chemical Society.

[19] Gregory J. Fiola, Dushyant M. Chaudhari, Stanislav I. Stoliarov, Comparison of pyrolysis properties of extruded and cast poly(methyl methacrylate), Fire Saf. J. 120 (2021) 103083.

[20] T. Kashiwagi, A. Inaba, J.E. Brown, Differences in PMMA degradation characteristics and their effects on its fire properties, Fire Saf. Sci. 1 (1986) 483–493.

[21] Talal Fateh, Franck Richard, Thomas Rogaume, Paul Joseph, Experimental and modelling studies on the kinetics and mechanisms of thermal degradation of polymethyl methacrylate in nitrogen and air, J. Anal. Appl. Pyrolysis 120 (2016) 423–433.

[22] Ho-Ming Tong, Augustus C. Ouano, Bubble formation mechanism during heat treatment of polymer films cast from solutions, Polym. Eng. Sci. 25 (2) (1985) 75–82.

[23] S.M. Dakka, TG/MS of poly (methyl methacrylate), the effect of heating rate on the rate of production of evolved gases, J. Therm. Anal. Calorim. 75 (3) (2004) 765–772.

[24] Röhm, Spektrale Transmissionsgrade $\tau(\lambda)$ im nahen Infrarot-Bereich bis 2,8 μm Wellenlänge.

[25] P. Gabbott, Principles and Applications of Thermal Analysis, Wiley, 2008.

[26] J.D. Menczel, R.B. Prime, Thermal Analysis of Polymers: Fundamentals and Applications, Wiley, 2014.

[27] J.A. Brydson, Plastics Materials, Elsevier Science & Technology, Oxford, United Kingdom, 1999.

[28] Philip J. Pritchard, Fox and McDonald's Introduction to Fluid Dynamics, eighth ed., John Wiled & Sons, Inc., Hoboken, 2011.

[29] B.A. Toms, D.J. Strawbridge, Elastic and viscous properties of dilute solutions of polymethyl methacrylate in organic liquids, Trans. Faraday Soc. 49 (1953) 1225.

[30] Ketan Pancholi, Eleanor Stride, Mohan Edirisinghe, Dynamics of bubble formation in highly viscous liquids, Langmuir 24 (8) (2008) 4388–4393, Publisher: American Chemical Society.